Available online www.jsaer.com

***Journal of Scientific and Engineering Research*, 2023, 10(5):57-68**

Research Article

ISSN: 2394-2630
CODEN(USA): JSERBR

Research on Parallel Braking Control of Distributed Drive Electric Vehicle

Chunming Zhao*

*School of Transportation and Vehicle Engineering, Shandong University of Technology, Shandong Province, Zibo, 255000, China

Abstract Aiming at the distributed drive electric vehicle, according to the actual demand of the composite braking system of the electric vehicle, the distributed parallel braking control strategy is proposed based on braking safety and energy recovery. The strategy adopts a hierarchical control structure. The upper control strategy aims to ensure the stability of vehicle braking during braking. The lower controller performs secondary distribution of motor braking torque on the basis of the upper control. The designed parallel braking control strategy considers the front and rear axle braking force distribution, battery SOC, charging power, motor external characteristics and slip rate. Finally, the simulation analysis is carried out to verify the braking efficiency and energy recovery effect.

Keywords Distributed electric vehicles ; Parallel braking ; Braking energy recovery

1. Introduction

During the braking process of the electric vehicle, the motor is changed from the motor mode to the generator mode. The inertia of the vehicle drives the rotor of the motor to rotate to generate a reverse torque. The direction of this torque is opposite to the direction of the speed, so that the mechanical braking torque is generated on the shaft to slow down the vehicle, while part of the kinetic energy is converted into electrical energy to charge the battery. According to the different combination of motor braking and hydraulic braking, the composite braking system is divided into two ways: series braking and parallel braking. The series composite braking system is to change the original hydraulic braking mechanism, increase the wire control system, control the hydraulic braking system, so that it can realize electronic control, cooperate with the motor braking of the driving wheel, and carry out composite braking in different working environments. Hydraulic braking and motor braking can achieve coordination during braking [1,2]. This composite braking system has high energy recovery efficiency, but the control and structure are complex, the required control accuracy is relatively high, and the cost of transformation is high. The parallel composite braking system is based on the original hydraulic braking structure to increase the motor braking torque on the driving wheel, and superimpose the electric mechanism power on the hydraulic braking force. Although the energy recovery effect of this composite braking system is general, it is relatively simple and easy to implement without transforming the original hydraulic braking system.

For the distributed two-wheel drive electric vehicle, Zhang et al. designed two parallel braking strategies and compared them with the series strategy [3,4]. The recovery rate of the series strategy is higher than that of the parallel strategy, but it is difficult to be used in engineering practice. At present, the parallel braking strategy is mostly used for centralized drive or distributed two-wheel drive electric vehicles. There are relatively few studies on four-wheel drive electric vehicles, and the parallel braking strategy is mostly compared with the parallel braking strategy for simulation and analysis. The lack of experimental comparison cannot verify the reliability of the simulation analysis results.

In this paper, a parallel composite braking system is designed for distributed drive four-wheel drive electric vehicles according to the real vehicle structure, battery SOC value, vehicle speed, motor and battery. At the same time, a simulation model is established in AMESim and Matlab and other related software to carry out

joint simulation to verify the braking performance and energy recovery effect of the composite braking control system.

2. Structure design of composite braking system

The parallel composite braking system uses the traditional hydraulic braking system and the motor braking system to work together [5]. The mechanical power of the hydraulic braking system comes from the traditional hydraulic brake. Four hub motors are equipped with a set of hydraulic brakes. Hydraulic brake system includes brake pedal, brake master cylinder disc brake and brake disc. As shown in Figure 1.

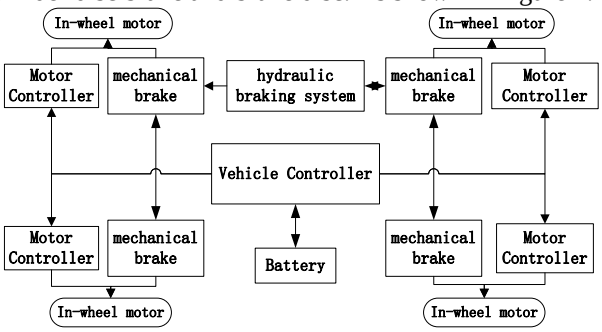

Figure 1: Structure scheme of composite braking system

3. Control strategy of composite braking system

3.1 Control strategy structure

The composite braking control strategy adopted by this vehicle is an improved control strategy based on the braking mode of traditional vehicles. The composite braking control strategy adopted by the laboratory vehicle is an improvement of the control strategy based on the hydraulic braking mode used by the traditional vehicle. The hierarchical control strategy of the composite braking system meets the braking requirements of the vehicle. The control strategy structure is mainly divided into two parts. The upper control strategy aims to ensure the stability of the vehicle braking during braking. According to the vehicle parameters during braking, a reasonable control algorithm is adopted to make the front and rear wheel braking force distribution as much as possible. The ideal front and rear brake force distribution curve is superimposed on the electric mechanism force on the basis of the wheel hydraulic braking force to control the braking torque, so as to ensure good stability in the vehicle braking process. The lower controller distributes the braking torque twice on the basis of the upper control, that is, the regenerative braking force of the motor is reasonably distributed for the purpose of braking energy recovery. According to the speed of the vehicle during braking, the characteristics of the motor itself and the operating state of the battery SOC, the power of the electric mechanism is constrained to achieve energy recovery during braking. In the braking process, the motor braking torque of the hub motor and the mechanical braking torque of the hydraulic braking system participate together, and energy recovery is carried out on the premise of ensuring braking stability. The overall structure of the hierarchical braking control strategy is shown in Figure 2.

As shown in the figure, the vehicle hierarchical braking control strategy, the upper control strategy mainly includes two-degree-of-freedom ideal vehicle model, yaw moment control module, braking strength identification module and each wheel torque distribution module. The two-degree-of-freedom vehicle model receives the vehicle speed signal V and the wheel angle signal δ to calculate the ideal yaw rate and the sideslip angle β. The yaw moment control module receives the difference e between the ideal yaw rate signal and the actual yaw rate signal, and uses the fuzzy control method to calculate the braking compensation yaw moment Mzd. The braking strength Z is obtained after identifying the input of the brake pedal, and the braking torque T required by the vehicle is calculated. After receiving the signal from each module, the wheel torque distribution module distributes the required braking torque to each wheel with the braking stability as the control target.

The lower control strategy aims at braking energy recovery and distributes the electric mechanism power. Although the more power distribution of the electric mechanism, the better the effect of energy recovery, due to the limitation of the characteristics of the motor itself, the speed of the vehicle, the SOC of the battery and the charging power, it is necessary to control the electric mechanism power, so that the electric mechanism power is superimposed with the hydraulic braking force without affecting the braking stability. In the case of conventional braking, energy recovery can be carried out under the premise of satisfying the stability of braking.

In the case of emergency braking and locking, the motor braking is abandoned, so as not to interfere with the hydraulic braking in the case of braking emergency and ensure the braking stability of the vehicle.

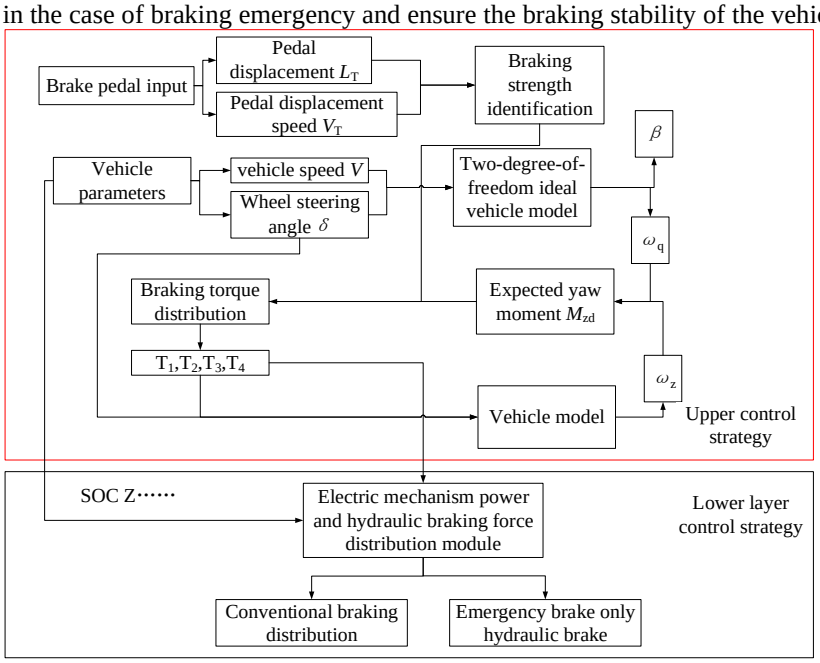

Figure 2: Control strategy structure

3.2 Braking force distribution

When the driver gives the braking signal through the brake pedal, it achieves different degrees of braking effect. When the braking strength is small, the maximum adhesion of the ground can overcome the friction braking force to make the wheel roll. With the increase of the braking strength, the maximum adhesion of the ground cannot meet the friction braking force, and the wheel is locked and skidded. In the braking process, the locking order of the front and rear wheels is affected by the distribution ratio of the braking force of the front and rear brakes and the conditions of the road adhesion [6-8].

In order to ensure the safety of the vehicle during braking without dangerous conditions, the vehicle should try to avoid locking when braking. When locking, the front and rear wheels should be locked at the same time or only the front wheels should be locked.

According to the braking force analysis of the electric vehicle, the braking force distribution of the front and rear wheels can be obtained as follows:

$$\begin{cases} F_{\mu 1} = \dfrac{Mg(b+zh_g)}{L} \\ F_{\mu 2} = \dfrac{1}{2}\left[\dfrac{Mg}{h_g}\sqrt{b^2+\dfrac{4h_gL}{Mg}F_{\mu 1}}-(\dfrac{Mgb}{h_g}+2F_{\mu 1})\right] \end{cases} \tag{1}$$

The basic parameters of the vehicle are brought into Formula 1, and the ideal braking force distribution curve I curve of the front and rear axles can be calculated. In order to avoid the situation that the rear wheel is first locked, the distribution curve of the front and rear braking force should appear below the I curve when the electric vehicle is braking. Therefore, the braking force curve equations of the front and rear wheels are shown in Formula 2:

$$F_{\mu 1}-\frac{1}{2}\left[\frac{Mg}{h_g}\sqrt{b^2+\frac{4h_gL}{Mg}}-(\frac{Mgb}{h_g}+2F_{\mu 2})\right]<0 \tag{2}$$

When the vehicle brakes under different ground adhesion coefficients, the braking force distribution formula of the front wheel lock is:

$$F_{\mu 2}-\frac{1}{2}\left[\frac{Mg}{h_g}\sqrt{b^2+\frac{4h_gL}{Mg}}-(\frac{Mgb}{h_g}+2F_{\mu 1})\right]=0 \tag{3}$$

At the same time, according to the requirements of ECE braking regulations for braking, when the braking strength z is 0.2-0.8, the constraints of the vehicle are $z \geq 0.1+0.85\times(\varphi-0.2)$. The braking force of the front and rear wheels should meet:

$$\begin{cases} F_{\mu 1} \leq \dfrac{Mgz(b+zh_g)}{L} \times \dfrac{z+0.7}{0.85} \\ F_{\mu 2} = Mgz - F_{\mu 1} \end{cases} \tag{4}$$

The critical curve M curve of ECE braking regulation can be obtained by Eq. (4):

$$\frac{(F_{\mu 1}+F_{\mu 2})^2 h_g}{MgL} + \frac{(F_{\mu 1}+F_{\mu 2})(0.07h_g+b)}{L} + \frac{0.07Mgb}{L} - 0.85F_{\mu 1} = 0 \tag{5}$$

The vehicle parameters are substituted into the formulas (3) and (5) to obtain the ideal front and rear axle braking force distribution curve I curve and the ECE regulation curve M curve when the vehicle is fully loaded. As shown in Figure 3, the area enclosed by the I curve and the M curve is the stable condition in which the vehicle will only have the front wheel locked under the limit condition of braking, and the braking force distribution area allowed by the ECE regulation.

The parameters of the vehicle are shown in Table 1:

Table 1: Vehicle parameters

Parameter	Numerical value
Full load mass	800kg
Front and rear wheelbase	2.35m
Height of center of mass	0.50m
The distance from the front axle to the center of mass	1.30m
The distance from the rear axle to the center of mass	1.05m
Tire radius	0.27m

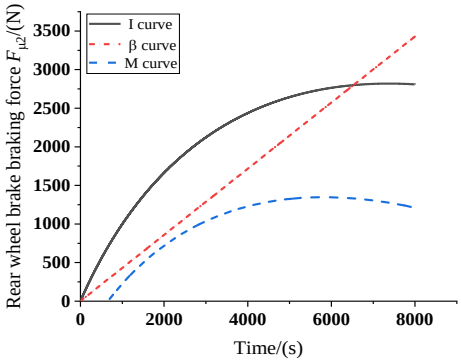

Figure 3: Braking force distribution graph

The distribution of front and rear axle braking should be as close as possible to the I curve, and the braking force of the front and rear wheel motors should be as close as possible to the I curve when the vehicle is braking straight. According to the ECE regulations for the braking regulations of M1 vehicles, the braking force distribution relationship between the front and rear wheels is stipulated, as shown in Figure 4.

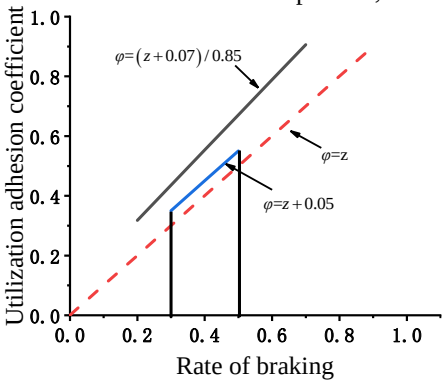

Figure 4: ECE regulatory requirements

The regulations stipulate that when the vehicle brakes on the road with the adhesion coefficient φ of 0.2 to 0.8, the braking strength of the vehicle should be $z \geq 0.1+0.85(\varphi-0.2)$, that is $\varphi \leq (z+0.07)/0.85$. In order to prevent the rear axle wheel from locking and slipping first, the regulations stipulate that the utilization adhesion coefficient of the rear axle must be lower than that of the front axle. When the braking strength is between 0.3 and 0.5, the utilization adhesion coefficient of the rear axle should not exceed the area of $\varphi = z+0.05$, and the utilization adhesion coefficient of the rear axle can be allowed to be above the utilization adhesion coefficient of the front axle.

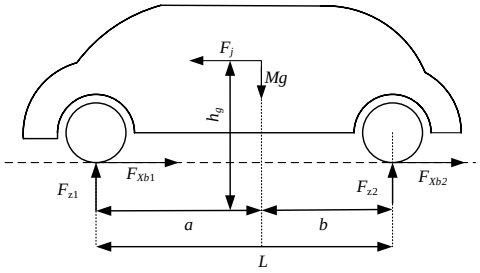

Figure 5: Braking force analysis diagram of the vehicle

According to the force analysis of the vehicle during braking in Figure 5, the utilization adhesion coefficient of the front wheel is :

$$\varphi_f = \frac{F_{xb1}}{F_{z1}} = \frac{\beta z L}{b + Z h_g} \tag{6}$$

The utilization adhesion coefficient of the rear wheel is :

$$\varphi_r = \frac{F_{xb2}}{F_{z2}} = \frac{(1-\beta) z L}{b + Z h_g} \tag{7}$$

At the same time, according to the requirements of ECE regulations, the relationship between the utilization adhesion coefficient of the front and rear wheels can be obtained :

$$\begin{cases} \varphi_r \leq z + 0.05 \\ \varphi_f \leq \dfrac{z+0.07}{0.85} \\ \varphi_f > \varphi_r \end{cases} \tag{8}$$

According to the relationship between the utilization adhesion coefficient of the front and rear wheels and the utilization adhesion coefficient of the front and rear wheels, the following inequality group can be formed, as shown in Formula (9) :

$$\begin{cases} \beta \geq \dfrac{b + z h_g}{L} \\ \beta \geq 1 - \dfrac{(z+0.07)(a - z h_g)}{0.85 z L} \\ \beta \leq \dfrac{(z+0.07)(b + z h_g)}{0.85 z L} \end{cases} \tag{9}$$

The control curves of the three braking force distribution coefficients are shown in Figure 6.

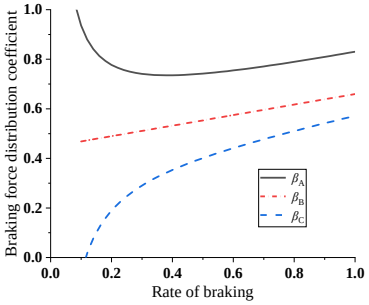

Figure 6: Curve of braking force distribution coefficient and braking strength

In Fig.6, β_A and β_C are the upper control line and the lower control line, respectively. β_B is the control line of the locking order, and the most suitable β range is in the region between β_A and β_C. In order to determine the distribution coefficient β value of the electric mechanism power, the minimum value of the equation of the β_A curve is determined as the maximum value of β, and the maximum value of the β_B curve is determined as the minimum value of β. The equation of the β_A curve in the diagram is:

$$\beta_A = \frac{(z+0.07)(b+zh_g)}{0.85zL} \tag{10}$$

Then the derivative is obtained and let the derivative value be 0, then the maximum value of β is

$$\beta_{max} = \frac{b\sqrt{\frac{0.07b}{h_g}} + 0.07(b + bh_g + \sqrt{0.07bh_g})}{0.85L\sqrt{\frac{0.07b}{h_g}}} \tag{11}$$

The equation of β_B curve in the figure is:

$$\beta_B = \frac{b+zh_g}{L} \tag{12}$$

The maximum value of β_B curve is:

$$\beta_{Bmax} = \frac{b+0.8h_g}{L} \tag{13}$$

Substituting the vehicle parameters in Table 1, the range of braking force distribution coefficient can be obtaine d:

$$0.6170 \le \beta \le 0.7359$$

At this time, the braking force of the vehicle is:

$$\begin{cases} F_{Bf} = F_{fl} + F_{fr} + F_{\mu y1} \\ F_{Br} = F_{rl} + F_{rr} + F_{\mu y2} \end{cases} \tag{14}$$

In the formula, F_{Bf} and F_{Br} are the braking force of the front and rear axles of the vehicle, F_{fl}, F_{fr}, F_{rl} and F_{rr} are the electric force of the left front, right front, left rear and right rear wheels of the vehicle, respectively, $F_{\mu y1}$ and $F_{\mu y2}$ are the hydraulic braking force of the front and rear axles of the vehicle, respectively. When the vehicle is braking, the power mechanism is superimposed on the basis of the hydraulic braking force, and the hydraulic braking force cannot be controlled by electronic control. The hydraulic braking system used by the vehicle is roughly close to the ideal braking force distribution curve to distribute the braking force of the front and rear axles, and the braking force on the left and right sides is equally divided. At the same time, because the braking force of the parallel composite braking is realized by the superposition of the electric mechanism power and the hydraulic braking force, so in order to ensure the safety and stability of the vehicle braking, the proportion of the electric mechanism power of the front and rear axles should be the same as that of the ideal front and rear wheels.

The desired yaw moment and front and rear braking force are:

$$M_{zd} \ge 0, \begin{cases} F_{fr} a \sin\delta + F_{fr}\cos\delta \dfrac{l_f}{2} + F_{rr}\dfrac{l_r}{2} = M_{zd} \\ F_{fl} = 0 \\ F_{rl} = 0 \\ \dfrac{F_{fr}}{F_{rr}} = \dfrac{F_{\mu 1}}{F_{\mu 2}} \end{cases} \tag{15}$$

$$M_{zd}<0,\begin{cases}F_{\mathrm{fl}}a\sin\delta-F_{\mathrm{fl}}\cos\delta\dfrac{l_f}{2}-F_{\mathrm{rl}}\dfrac{l_r}{2}=M_{zd}\\F_{\mathrm{fr}}=0\\F_{\mathrm{rr}}=0\\\dfrac{F_{\mathrm{fr}}}{F_{\mathrm{rl}}}=\dfrac{F_{\mu 1}}{F_{\mu 2}}\end{cases}\tag{16}$$

In the formula, l_{f} and l_{r} are the distance between the left and right wheels of the front axle of the vehicle and the distance between the left and right wheels of the rear axle.

3.3 Parallel braking constraints

The proposed parallel braking strategy takes into account the battery SOC, motor operating characteristics, battery charging power and slip rate, and limits the power of the electric mechanism.

(1) Battery SOC

The current generated by the electric braking when the vehicle is braking needs to be recycled into the power battery. Therefore, whether energy recovery can be performed first depends on the SOC of the battery. In order to prevent the electric energy generated during the braking process from overcharging the battery, The motor braking force needs to be constrained. Therefore, the SOC value of the battery is set to 0.85 when the motor is braking, and the electric braking is stopped when the SOC value is greater than 0.85. The battery SOC influence factor K_{soc} is set as:

$$K_{soc}=\begin{cases}0\,|\,soc>85\%\\20(0.85-soc)\,|\,80\%\le soc\le 85\%\\1\,|\,80\%>soc\end{cases}\tag{17}$$

(2) Motor external characteristic curve

The braking torque of the motor changes with the external characteristic curve of the motor, as shown in Figure 7. When the motor can work in the constant power or constant torque region at different speeds, when the controller distributes the electric mechanism power, the regenerative braking torque generated by the motor should not exceed the maximum braking force that the motor can provide.

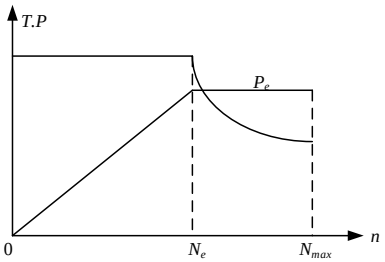

Figure 7: Motor external characteristic curve

The maximum torque that the motor can achieve at different speeds is:

$$T_{m\max}=\begin{cases}T_e\,|\,n\le N_e\\\dfrac{9550P_e}{n}\,|\,n>N_e\end{cases}\tag{18}$$

In the formula,T_{e} is the peak torque of the motor, and the unit is N ; P_{e} is the peak power of the motor, and the unit is kW ; n is the motor speed, the unit is r / min ; N_{e} is the rated speed of the motor, the unit is r / min.

The maximum regenerative braking force that the motor can produce is:

$$F_{m\max}=\frac{T_{m\max}i_g i_0\eta_T}{r}\tag{19}$$

In the formula, η_T is the mechanical transmission efficiency and r is the wheel radius.

At the same time, according to the transmission characteristics of the transmission system, the relationship between motor speed and vehicle speed is :

$$n = \frac{v i_g i_0}{0.377 r} \tag{20}$$

In the formula, v is the vehicle speed, i_g is the transmission ratio of the transmission, i_0 is the transmission ratio of the main reducer.

It can be seen from Formula 10 that the vehicle speed is proportional to the speed of the motor, and the vehicle speed directly affects the maximum torque of the motor. When the speed of the vehicle is less than 10km/h, according to the formula, the speed of the motor is reduced. When the vehicle is braked, the inertia of the vehicle itself is small, and the back electromotive force higher than the battery voltage cannot be generated, so that the regenerative braking ability disappears. Therefore, when the speed is less than 10km/h, the motor braking is not involved in the braking process, and only the hydraulic braking is performed. Setting the speed influence factor as K_v

$$K_v = \begin{cases} 0 \mid v \le 10\text{km/h} \\ 1 \mid v > 10\text{km/h} \end{cases} \tag{21}$$

(3) Charging power

The rechargeable power generated by a single motor when the vehicle is braking is:

$$P_b = \eta_M \times \eta_i \times \eta_B \times P_{m\max} \tag{22}$$

In the formula, P_b is the instantaneous power during charging, η_M is the power generation efficiency of the motor, η_i is the inverter efficiency, η_B is the charging efficiency of the battery, and P_{mmax} is the maximum power generation efficiency of the battery.

The total power when all motors are electrically braked is:

$$P_{batt} = \sum P_b \tag{23}$$

The braking current generated by the motor braking is:

$$I = \frac{P_{batt}}{U} \tag{24}$$

The instantaneous power and charging current generated by charging during the motor braking process should not be greater than the maximum rated charging power and rated charging current of the battery to prevent damage to the battery. The charging power influencing factor K_p and the charging current influencing factor K_I are set as:

$$K_p = \begin{cases} 0 \mid P_{batt} > P_e \\ 1 \mid P_{batt} \le P_e \end{cases} \tag{25}$$

$$K_I = \begin{cases} 0 \mid I > I_e \\ 1 \mid I \le I_e \end{cases} \tag{26}$$

Among them, P_e is the rated charging power, and I_e is the rated charging current.

(4) Slip rate

Through a large number of experimental studies and theoretical analysis, when the slip ratio of the vehicle is in the range of 18 % to 20 %, the vehicle can obtain good braking performance, and different road surfaces have different optimal slip ratios. Therefore, the vehicle generally sets 18 % to 20 % as the slip ratio control target during braking, thus stabilizing the vehicle in the stable area. Because the hydraulic brake is uncontrollable, the superimposed electric mechanism force will have the risk of locking the wheel. When the vehicle is locked, the electric mechanism force needs to be reduced to 0, reducing the braking force and improving the stability of the vehicle. At the same time, in order to enable the hydraulic brake to perform anti-lock braking. Therefore, the risk coefficient KS is set. When the vehicle brakes, $K_S = 0$; when the vehicle does not brake, $K_S = 1$.

Through the above analysis, the maximum value of the actual power of the electric mechanism can be obtained:

$$F_{\text{mmax}} = \frac{T_{\text{mmax}} i_g i_0 \eta_T K_v K_P K_I K_{soc} K_s}{r} \tag{27}$$

4. Simulation Analysis

The distributed parallel braking control simulation model of electric vehicle is built by using AMESim and Matlab / Simulink and two software. AMESim model includes vehicle dynamics model, wheel model, battery model, motor model and hydraulic braking model. The AMESim model software interface receives the four-wheel motor braking torque and the four-wheel hydraulic braking torque to obtain the remaining SOC value, power, motor speed, vehicle speed, sideslip angle and yaw rate of the vehicle for the control module to call.

The Simulink model includes a steering wheel angle input module, a braking strength identification module, a yaw moment compensation module, a two-degree-of-freedom ideal vehicle model, and an electrical power distribution module. The model determines the electric mechanism power and hydraulic braking force of each wheel according to the designed composite braking control strategy, so that the vehicle can maximize the energy recovery while ensuring the braking stability of the vehicle.

(1) Low adhesion braking

The conditions of the selected simulation conditions are the ground with a adhesion coefficient of 0.3, the displacement and speed of the brake pedal change a certain, and the braking strength is the same. The identified 0.2 braking strength is used to brake at the initial speeds of 30km/h, 60km/h and 90km/h, respectively. The obtained speed change curve is shown in Figure 8, the acceleration change curve is shown in Figure 9, and the braking distance change curve is shown in Figure 10.

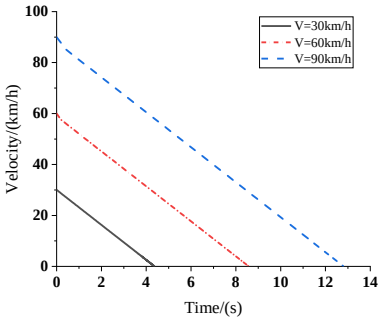

Figure 8: Speed change curve

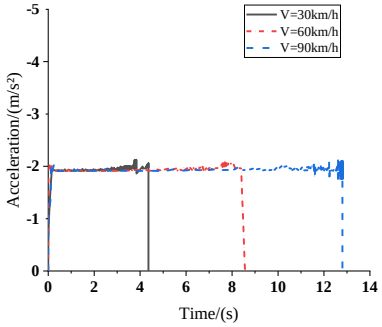

Figure 9: Acceleration curve curve.

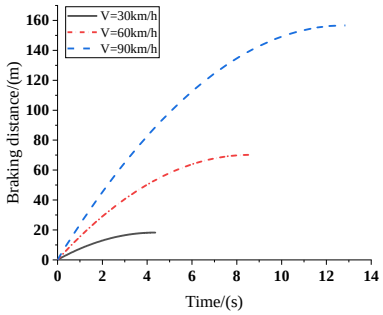

Figure 10: Braking distance change curve

It can be seen from Figure 8 that the braking time under three different initial braking speeds is 4.3s, 8.3s and 12. 1s respectively ; due to the effect of motor braking superimposed on hydraulic braking force, the braking respon se is faster and the braking starts in a short time. The braking distances of the three speeds are 18.2m, 70.12m an d 156.63m respectively. Because of the low braking strength and the small ground adhesion coefficient, the brak ing distance is relatively long. The slip change rate and SOC change of the four wheels at three different speeds are shown in Figure 11, Figure 12, Figure 13 and Figure 14, respectively.

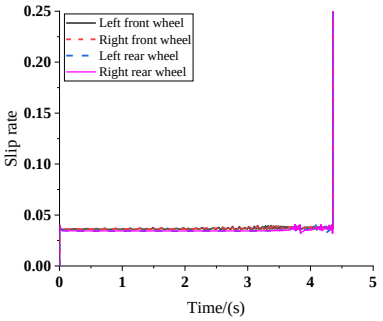

Figure 11: 30km/h slip rate change curve

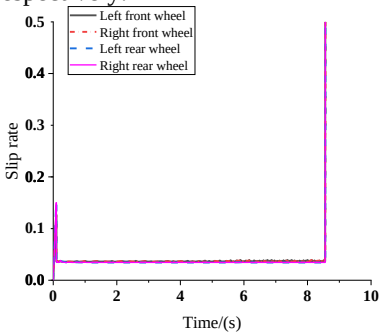

Figure 12: 60km/h slip rate change curve

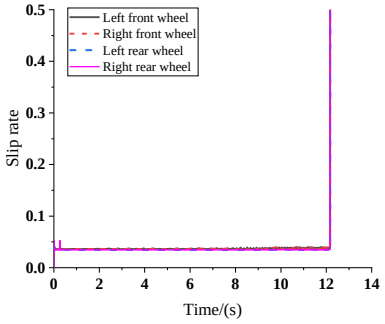

Figure 13: 90km/h slip rate change curve

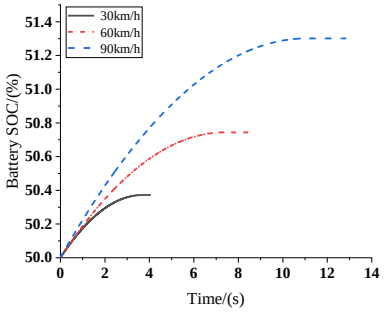

Figure 14: SOC change curve.

Under the three initial braking speeds, when the vehicle is braking in a straight line, the slip rate of the four wheels is maintained at about 0.025, and there is no wheel lock state. In addition, except for the initial stage of braking, the slip rate curve fluctuates briefly, and the rest time slip rate remains basically stable, which proves that the composite braking system works well. Because the input pedal displacement and displacement change speed are the same, the braking strength is the same, so the braking force of the front and rear axles of the vehicle is the same. The braking torque and hydraulic braking torque of the front and rear axle motors remain unchanged at three different initial speeds. The electric mechanism power gradually increases and then continues to participate in braking, so the battery SOC continues to increase. As the speed slows down, the battery SOC growth rate slows down until the speed drops to 0.

(2) High adhesion braking

The conditions set by the selected simulation conditions are the ground with an adhesion coefficient of 0.7, the displacement and speed of the brake pedal are constant, and the braking strength is the same. The braking strength of about 0.5 is used to brake at the initial speeds of 30km/h, 60km/h and 90km/h, respectively. The obtained speed curve, acceleration curve and braking distance curve are shown in Figure.15, Figure.16 and Figure17.

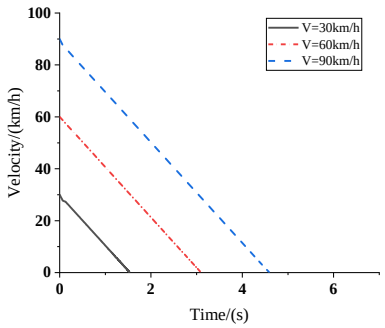

Figure 15: Speed change curve

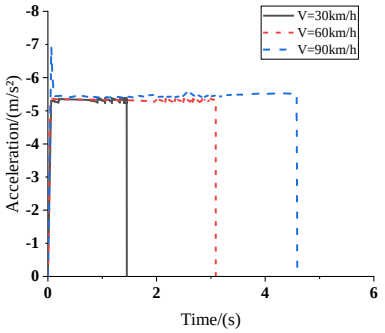

Figure 16: Acceleration curve curve.

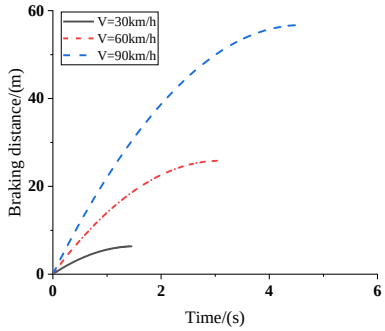

Figure 17: Braking distance change curve

The obtained speed change curve is shown in Figure.15. The braking time at three different initial speeds is 1.43s, 3.13s and 4.61s, respectively. The acceleration change curve is shown in Figure 16. Because the motor braking is superimposed on the hydraulic braking force, the braking response is faster and the braking starts in a short time. The braking distance curve is shown in Figure.17. The braking distances of the three speeds are 6.32 m, 25.8 m and 56.71 m respectively. Because of the large ground adhesion coefficient and the increase of

braking force, the braking distance is relatively close. The slip change rate and SOC change of the four wheels at three different speeds are shown in Figure 18, Figure 19 Figure 20 and Figure 21 respectively.

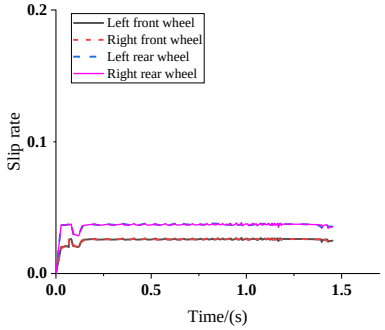

Figure 18: 30km/h slip rate change curve

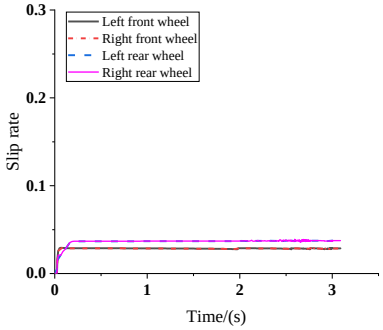

Figure 19: 60km/h slip rate change curve

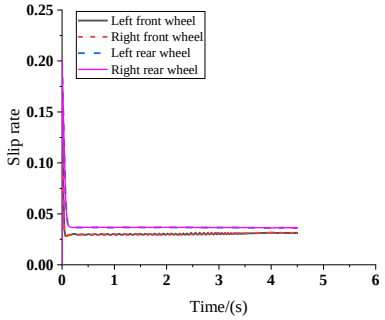

Figure 20: 90km/h slip rate change curve

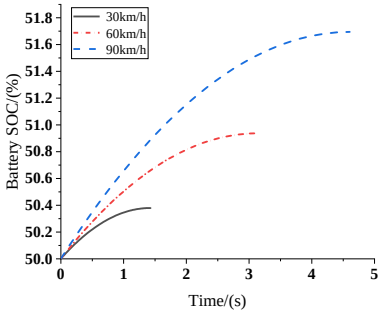

Figure 21: SOC change curve.

Under the three initial braking speeds, when the vehicle is braking in a straight line, the slip rate of the four wheels is maintained below 0.05, and there is no wheel locking state. In addition to the initial stage of braking, the slip rate curve of 30km/h and 60km / h braking appears a short small fluctuation, and the slip rate curve of 90km / h braking appears a short fluctuation close to 0.2 slip rate, and the slip rate remains basically stable at the rest of the time. It is proved that the composite braking system can brake in time during the braking process, maintain stability and control effect is good. Because the braking strength is the same, the braking force of the front and rear axles of the vehicle is the same, so the front and rear axle motor braking torque and hydraulic braking torque remain unchanged at three different initial speeds. The power of the electric mechanism gradually increases and then continues to participate in the braking, so the battery SOC increases continuously. As the vehicle speed slows down, the growth rate of the battery SOC slows down until the vehicle speed drops to 0.

5. Conclusion

In this paper, a hierarchical control parallel braking control strategy is adopted for distributed four-wheel drive electric vehicles considering braking stability and safety. The simulation model of distributed parallel braking control is built by AMESim and Simulink software. The braking stability of the vehicle under low adhesion and high adhesion is simulated and analyzed. The speed change, braking distance, acceleration change, slip rate change and battery SOC value change curve of the vehicle under two different braking conditions are obtained. It can be concluded that the distributed parallel braking control strategy has braking stability and can recover braking energy.

References

[1]. Gu Yu, He Ren, Wang Juncheng. (2020). Coordinated control strategy of in-wheel motor electric vehicle regenerative hydraulic compound braking system [J]. *Journal of Chongqing University of Technology: Natural Science, 34(6)*, 32-40.

[2]. Zhang S Q, Liu R L, Liu W Q, et al. (2014). Steady flow characteristics of 4-valve gasoline engine with variable valve dissimilitude lift [J]. *Transactions of Csice, 32(1)*, 57-63.

[3]. Guo Jingang, Dong Haoxuan, Sheng Weihui, et al. (2018). Optimal control strategy for regenerative braking energy recovery of electric vehicles [J]. *Journal of Jiangsu University: Natural Science Edition, 39(2)*, 132-138.

[4]. Zhang Kangkang, Xu Liangfei, Hua Jianfeng, et al. (2015). Comparative study on braking energy recovery systems and strategies of rear-wheel-drive pure electric vehicles [J]. *Automotive Engineering, 37(2)*, 125-131, 138.

[5]. Zhu Shaopeng, Lin Ding, Xie Bozhen, et al. (2016). Hierarchical control strategy of electric vehicle driving force [J]. *Journal of Zhejiang University: Engineering Science, 50(11)*, 2094-2099.

[6]. Tian Shaopeng, Lv Chenyang. (2018). Research on regenerative braking strategy of pure electric vehicle based on fuzzy control [J]. *Logistics Technology, 37(08)*, 92-97+121.

[7]. Zhang S, Zhang X, Wang H, et al. (2014). Study on Air Flow Characteristics in Cylinders of a Four-Valve Engine with Different Lifts of Valves [J]. *Open Mechanical Engineering Journal, 8(1)*, 185-189.

[8]. Huang Xueyan, Li Yunwu, Liu Dexiong, et al. (2018). Braking energy recovery control strategy of four-wheel independent drive electric vehicle [J]. *Science Technology and Engineering, 18(10)*, 167-173.